Research Article | Vol. 30, No. 20 / 26 Sep 2022 / Optics Express 35840
Optics EXPRESS

Quantum analog of the maximum power transfer theorem

CRISTIAN L. CORTES, WENBO SUN, AND ZUBIN JACOB*

Birck Nanotechnology Center, Elmore Family School of Electrical and Computer Engineering, Purdue University, West Lafayette, Indiana 47907, USA
*zjacob@purdue.edu

Abstract: We discover the quantum analog of the well-known classical maximum power transfer theorem. Our theoretical framework considers the continuous steady-state problem of coherent energy transfer through an N-node bosonic network coupled to an external dissipative load. We present an exact solution for optimal power transfer in the form of the *maximum power transfer theorem* known in the design of electrical circuits. Furthermore, we introduce the concept of quantum impedance matching with Thevenin equivalent networks, which are shown to be exact analogs to their classical counterparts. Our results are applicable to both ordered and disordered quantum networks with graph-like structures ranging from nearest-neighbor to all-to-all connectivities. This work points towards universal design principles adapting ideas from the classical regime to the quantum domain for various quantum optical applications in energy-harvesting, wireless power transfer, and energy transduction.

© 2022 Optica Publishing Group under the terms of the Optica Open Access Publishing Agreement

1. Introduction

In classical electrical circuit design, the maximum power transfer theorem states that in order to deliver maximum power to a load from a source with finite internal impedance, Z_s, the load must be designed to have an impedance, Z_l, that is equal to the conjugate impedance of the source, $Z_l = Z_s^*$. This concept known as conjugate impedance matching ensures maximum power delivery to the load. For a classical circuit consisting of a source, an internal network, and a load, Thevenin's theorem can be used to replace the entire network by a single effective source with an effective internal impedance, Z_{th}, resulting in the conjugate impedance matching condition, $Z_l = Z_{th}^*$. This theorem is a textbook example of an engineering principle that guides the design of electrical circuits, transmission lines, and classical wireless communication networks [1–3]. This principle is often used to maximize the transmission of classical information through a communications network since optimal signal delivery requires a signal with maximum strength at the receiving end. It is natural to ask whether similar guiding principles exist for quantum and nanoscopic systems. In this work, we answer this question affirmatively showing that this engineering principle, typically used in classical circuit design, is also applicable for a wide range of bosonic quantum systems, e.g. photons, phonons, and magnons. This points to important universal design principles for different types of networks, including networks of donors and acceptors in QED chemistry [4–14] and quantum optical networks of optical fiber cavity [15,16] with applications in energy transduction, energy transport in turbid media, and energy harvesting [1,2,15–28]. We note that the concept of maximizing energy transfer is different from the widely studied problem of quantum information transfer from a sender to a receiver with maximum fidelity [29].

In this work, we develop a unified framework, based on the Lindblad master equation, describing power delivery in dissipative quantum networks. We introduce an N-node coupled bosonic system that is coupled to an external dissipative load, shown in Fig. 1, as the quantum analog of a classical network. Physically, the quantum network can be thought of as a system of coupled optical cavities or waveguides or, alternatively, as a system of coupled two-level

#465020 https://doi.org/10.1364/OE.465020
Journal © 2022 Received 24 May 2022; revised 3 Aug 2022; accepted 30 Aug 2022; published 15 Sep 2022

Optics EXPRESS

systems operating in the single-excitation regime [7,30,31]. The load can be thought of as an outcoupling fiber, waveguide, or an external detector. We show that the problem of optimizing the power delivered to the load can be understood through a quantum version of the maximum power transfer theorem resulting in the intuitive conjugate impedance matching condition with effective non-Hermitian Hamiltonians as opposed to classical impedances. In simple form, we state the quantum maximum power transfer theorem as follows:

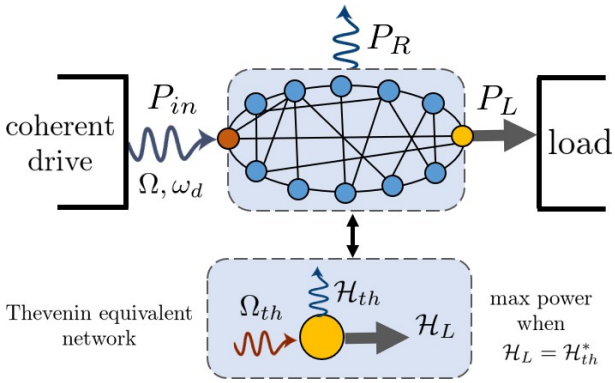

Fig. 1. Power transfer model through a dissipative quantum network described by non-Hermitian Hamiltonian $\mathcal{H}_{eff}$ (top) with Thevenin equivalent network (bottom). Maximum power transfer occurs when the non-Hermitian Hamiltonian of the load is conjugately matched with the Thevenin equivalent Hamiltonian, $\mathcal{H}_{th}$. The load may represent an outcoupling fiber, waveguide, or a detector.

A load connected to a linear dissipative quantum network receives maximum power when the load Hamiltonian H_L is conjugately matched to the Thevenin equivalent Hamiltonian H_{th} of the network such that, $H_L = H_{th}^*$.

Our introduction of the Thevenin-equivalent Hamiltonian arises naturally from the bosonic properties of the network, described by the Hamiltonian in Eq. (1), which contributes to coherent-like dynamics and power effects. The dissipative, non-Hermitian, contribution is captured by Lindblad-like dissipative terms in the quantum optical master equation (Eq. (2)). The results of this manuscript are valid in the weak and strong coupling regimes thereby taking into account the possibility hybridization between strongly coupled sites. We also show that the theorem applies to both ordered or disordered networks with graph-like structures ranging from nearest-neighbor connectivity to all-to-all connectivity applicable in both the incoherent and quantum coherent energy transfer regimes.

2. Description of dissipative quantum network

We consider a general model of power transfer through a bosonic quantum network described by the bare Hamiltonian ($\hbar = 1$),

$$H = \sum_n (\omega_n + \delta\omega_n)\hat{a}_n^\dagger \hat{a}_n + \sum_{n,m} J_{nm}\hat{a}_n^\dagger \hat{a}_m + \sum_n \Omega_n \hat{a}_n e^{i\omega_d t} + \text{h.c.} \tag{1}$$

The bosonic excitation is described by the operator $\hat{a}_n^\dagger$ ($\hat{a}_n$) which creates (destroys) a boson at site n with frequency $\tilde{\omega}_n = \omega_n + \delta\omega_n$, satisfying the commutation relations, $[a_n, a_m^\dagger] = \delta_{nm}$. $\delta\omega_n$ represents a frequency shift, a so-called Lamb shift, arising from coupling to the load. The excitation travels through the network with hopping amplitude J_{nm} between the nth and mth nodes. The network nodes are driven by a coherent driving field with frequency ω_d and drive amplitudes Ω_n.

Optics EXPRESS

Treating dissipation perturbatively in the Born-Markov limit, the time dynamics of the density operator ρ is described by the Lindblad master equation,

$$\dot{\rho} = -i[H, \rho] + \mathcal{D}_R[\rho] + \mathcal{D}_L[\rho]. \tag{2}$$

The first term on the right represents the coherent evolution of the total system. The second term, $\mathcal{D}_R[\rho]$, describes undesirable dissipation of the network to a background reservoir. The last term, $\mathcal{D}_L[\rho]$, describes dissipation into an external load. Both terms are explicitly written in terms of the Lindblad superoperators,

$$\mathcal{D}_R[\rho] = \sum_n \gamma_n (\hat{a}_n \rho \hat{a}_n^\dagger - \frac{1}{2}\{\hat{a}_n^\dagger \hat{a}_n, \rho\}), \tag{3}$$

$$\mathcal{D}_L[\rho] = \sum_n \Gamma_n (\hat{a}_n \rho \hat{a}_n^\dagger - \frac{1}{2}\{\hat{a}_n^\dagger \hat{a}_n, \rho\}). \tag{4}$$

The decay rate γ_n refers to the decay rate of the nth node to the undesirable reservoir, while Γ_n represents the decay rate from the nth node to the load. Throughout this manuscript, we work in regimes where $\gamma_n, \Gamma_n \ll \omega_n$ and memory effects in background bath and load reservoir can be neglected, consistent with the Born-Markov approximation [32]. The derived results for the maximum power transfer theorem are therefore only valid when these conditions remain true. Further considerations would be required to account for either strong couplings between nodes and reservoirs or non-Markovian effects due to the background and load reservoirs.

3. Power and efficiency

The power flow through the system is obtained from the Hamiltonian equation of motion, $\partial_t \langle H \rangle = \mathrm{tr}(\dot{H}\rho) + \mathrm{tr}(H\dot{\rho}) = P_{in} - P_{out}$ [33,34] (also see Appendix A). Under steady-state conditions, $\partial_t \langle H \rangle = 0$, the quantum network satisfies the power balance relation, $P_{in} = P_{out}$. The input power $P_{in} = \mathrm{tr}(\dot{H}\rho)$ represents power coupled into the network and is given by

$$P_{in} = i\omega_d \sum_n [\Omega_n \langle a_n \rangle e^{i\omega_d t} - \Omega_n^* \langle a_n^\dagger \rangle e^{-i\omega_d t}]. \tag{5}$$

The output power is divided into two major contributions, $P_{out} = P_R + P_L$, corresponding to power dissipated to the background reservoir, $P_R = \mathrm{tr}\,(H\mathcal{D}_R[\rho])$ and the power delivered to the load, $P_L = \mathrm{tr}\,(H\mathcal{D}_L[\rho])$. As shown in the Appendix A, these equations can be written in the following form,

$$P_R = \tfrac{1}{2} \sum_{n,m} (\gamma_n + \gamma_m) \left[\omega_{nm} \langle a_n^\dagger a_m \rangle + \Delta_{nm} \langle a_n^\dagger \rangle \langle a_m \rangle \right], \tag{6}$$

$$P_L = \tfrac{1}{2} \sum_{n,m} (\Gamma_n + \Gamma_m) \left[\omega_{nm} \langle a_n^\dagger a_m \rangle + \Delta_{nm} \langle a_n^\dagger \rangle \langle a_m \rangle \right], \tag{7}$$

where $\Delta_{nm} = \delta_{nm}(\omega_d - \tilde{\omega}_n + J_{nm}) - J_{nm}$. We emphasize that the equations above are more general than typical power expressions derived from classical coupled mode theory. Classical power typically depends only on the squared amplitude of a particular mode; these expressions include the contribution from off-diagonal coherences ($n \neq m$) [35]. The above equations represent one of the major contributions of this paper and will be subject to further investigation in the future. In the following, we consider power transfer in the absence of either dephasing or an incoherent pump such as a thermal bath. The coherent drive implies the factorization condition, $\langle a_n^\dagger a_m \rangle = \langle a_n^\dagger \rangle \langle a_m \rangle$, is exact under steady-state conditions. This can be readily confirmed by comparing Eqs. (29) and (30) in Appendix B. In this limit, all relevant observables can be written

Optics EXPRESS

in terms of the field amplitudes, $\langle a_n \rangle$. Accordingly, the radiated and load power simplify to (see Appendix B for more details)

$$P_R = \omega_d \sum_n \gamma_n \langle a_n^\dagger \rangle \langle a_n \rangle, \tag{8}$$

$$P_L = \omega_d \sum_n \Gamma_n \langle a_n^\dagger \rangle \langle a_n \rangle. \tag{9}$$

As expected from the dynamics of classically coupled harmonic oscillators, the radiated and load power are proportional to the driving frequency. Finally, we define the energy transfer efficiency as

$$\eta = \frac{P_L}{P_{in}} = \frac{P_L}{P_L + P_R}, \tag{10}$$

representing the percentage of power transferred into the load.

4. Thevenin equivalent network

We now show that when a single node, denoted as the Nth node, is connected to the load with all other nodes having zero coupling to the load, it is possible to rewrite the equations of motion for the N-node network as a *single-node* Thevenin equivalent equation of motion. As we show in the next section, this will allow the solution of the maximum power transfer problem to be understood as an intuitive impedance matching condition. To demonstrate the existence of a Thevenin equivalent network, we first write the equations of motion for the field amplitudes in matrix form (see Appendices B and C),

$$i\boldsymbol{\Omega}^* = (\tilde{\boldsymbol{\mathcal{H}}}_R + \boldsymbol{\mathcal{H}}_L)\tilde{\mathbf{a}}, \tag{11}$$

where the matrix elements of the non-hermitian matrix $\tilde{\boldsymbol{\mathcal{H}}}_R$ are $[\tilde{\boldsymbol{\mathcal{H}}}_R]_{nm} = i\delta_{nm}(\omega_d - \omega_n + J_{nm}) - iJ_{nm} - \delta_{nm}\gamma_n/2$, $\boldsymbol{\Omega}^* = (\Omega_1^*, \ldots, 0)^T$, and $\tilde{\mathbf{a}} = (\langle \tilde{a}_1 \rangle, \ldots, \langle \tilde{a}_N \rangle)^T$. Here, the tilde represents a transformation into the rotating frame of the driving laser field. We also introduce $\boldsymbol{\mathcal{H}}_L$ as a diagonal matrix representing the non-Hermitian coupling from the Nth node to the load with a single non-zero diagonal element, $[\boldsymbol{\mathcal{H}}_L]_{NN} = -i\delta\omega_N - \Gamma_N/2$. Equation (11) can be derived from the Lindblad master Eq. (2) (see Appendices B and C for derivations). In Eq. (11), dissipation into the environmental bath and load reservoir is contained in $\tilde{\boldsymbol{\mathcal{H}}}_R$ and $\boldsymbol{\mathcal{H}}_L$ respectively. Repetitive back substitution in this matrix equation produces the following steady-state equation for the N-th node,

$$i\Omega_{th}^{(N)} = \tilde{\mathcal{H}}_{th}\langle \tilde{a}_N \rangle + [\boldsymbol{\mathcal{H}}_L]_{NN}\langle \tilde{a}_N \rangle. \tag{12}$$

This equation defines the Thevenin equivalent representation of the quantum network. $\tilde{\mathcal{H}}_{th}$ is interpreted as the Thevenin equivalent energy of the network (as seen the Nth node). Using the Sherrman-Morrison formula [36], the explicit expression for the Thevenin equivalent energy may be written as:

$$\tilde{\mathcal{H}}_{th} = -i\delta\tilde{\omega}_{th} - \Gamma_{th}/2 = (\mathbf{e}_N^T \tilde{\boldsymbol{\mathcal{H}}}_R^{-1} \mathbf{e}_N)^{-1}. \tag{13}$$

Interestingly, this shows how the non-Hermitian Hamiltonian of open quantum systems plays an analogous role to complex impedance in macroscopic electrical circuits. The Thevenin equivalent energy is the quantum network generalization of the Thevenin impedance.

We also define the Thevenin equivalent drive amplitude, $\Omega_{th}^{(N)}$, as

$$\Omega_{th}^{(N)} = \frac{\mathbf{e}_N^T \tilde{\boldsymbol{\mathcal{H}}}_R^{-1} \boldsymbol{\Omega}^*}{\mathbf{e}_N^T \tilde{\boldsymbol{\mathcal{H}}}_R^{-1} \mathbf{e}_N}, \tag{14}$$

representing the effective amplitude that drives the Nth node. In the equations above, we introduced the unit vector $\mathbf{e}_N = (0, 0, \ldots, 1)^T$ for the last node.

Optics EXPRESS

In summary, we have shown that the quantum network can be re-written as an equivalent single-node network with equivalent driving field (Thevenin drive amplitude) and equivalent non-Hermitian Hamiltonian (Thevenin energy) for the Nth node. These results are applicable to driven-dissipative N-node quantum networks with arbitrary couplings and graph-like structures.

5. Maximum power transfer theorem

Following the results from the previous two sections, the power delivered to the load is: $P_L = \omega_d \Gamma_N \langle a_N^\dagger \rangle \langle a_N \rangle$. The Thevenin equivalent representation implies the general solution for the power delivered to the load is:

$$P_L = \omega_d \Gamma_N \frac{|\Omega_{th}|^2}{|\tilde{\mathcal{H}}_{th} + \mathcal{H}_L|^2}. \tag{15}$$

The maximum power delivered to the load is then found by optimizing the load's induced frequency shift $\delta\omega_N$ and decay rate Γ_N, using $\frac{\partial P_L}{\partial \delta\omega_N} = 0$ and $\frac{\partial P_L}{\partial \Gamma_N} = 0$. After some algebra, we find that the maximum power that can be delivered to the load occurs when

$$\delta\omega_N = -\delta\tilde{\omega}_{th} \quad \text{and} \quad \Gamma_N = \Gamma_{th}, \tag{16}$$

or equally,

$$\mathcal{H}_L = \tilde{\mathcal{H}}_{th}^*. \tag{17}$$

This condition is the quantum generalization of *conjugate impedance matching* that is well-known in circuit theory. Note that the quantum impedance matching condition depends only on the non-Hermitian Hamiltonian parameters of the quantum network and is not dependent on the driving field Rabi frequency, Ω_1, due the linearity of the quantum network. When quantum conjugate impedance matching is satisfied, the maximum power delivered to the load is found to be exactly equal to:

$$P_{L,max} = \hbar\omega_d \frac{|\Omega_{th}|^2}{\Gamma_{th}}. \tag{18}$$

Equations (17) and (18) form the main results of this manuscript. From this expression, it is clear that quantum networks with a large Thevenin Rabi frequency Ω_{th} and small Thevenin dissipative term, Γ_{th}, are ideal for enabling large power transfer rates. This can be used as an important rule of thumb for the efficient design of quantum power networks.

6. Energy transfer efficiency

While the conjugate impedance matching condition Eq. (17) ensures maximum power transfer, it does not guarantee maximum energy transfer efficiency. This result is exactly analogous to the classical case in electrical circuits. The exact form for the energy transfer efficiency is given by:

$$\eta = \frac{\Gamma_N |\langle a_N \rangle|^2}{\sum_n \gamma_n |\langle a_n \rangle|^2 + \Gamma_N |\langle a_N \rangle|^2}. \tag{19}$$

It is worth noting that we could not find a simple expression for the energy transfer efficiency in terms of the single-node Thevenin equivalent network representation. Instead, we introduced an equivalent two-node representation between the first and Nth node of the network (see appendix for details). In the limit of large effective coupling, H_{1N}, between the first and last nodes, the energy transfer efficiency is limited primarily by the intrinsic dissipative loss of the Nth node, γ_N. Perhaps more importantly, it is also possible to prove that the energy transfer efficiency, when the impedance matching condition is satisfied, will always be less than or equal to fifty percent. This demonstrates the existence of a fundamental trade-off between the maximum power that can be delivered to the load and the energy transfer efficiency.

Optics EXPRESS

7. Discussion

In Fig. 2, we present full numerical simulations for three distinct quantum networks including: (a) a simple 2-node network, (b) a 50-node 1-dimensional chain with nearest-neighbor coupling, and (c) a 50-node network with random all-to-all connectivity. The hopping parameters J_{nm} of the 50-node random network are sampled from a normal distribution with zero mean $J_{avg} = 0$ and standard deviation $J_{std} = 2\gamma_o$. To characterize different quantum networks, we use the network spectral density, $S(\omega_d) = \mathrm{Im}[\mathrm{tr}(\omega_d - \mathcal{H})^{-1}]$, which is closely related to the transmission amplitude which is well-known in input-output theory [37]. Ordered and disordered quantum networks can have distinct distributions of multiparty entanglement, which are closely related to the capacity of information transmission [38,39]. Here, we show that our theorem is applicable to ordered and disordered quantum networks with graph-like structures in Fig. 2.

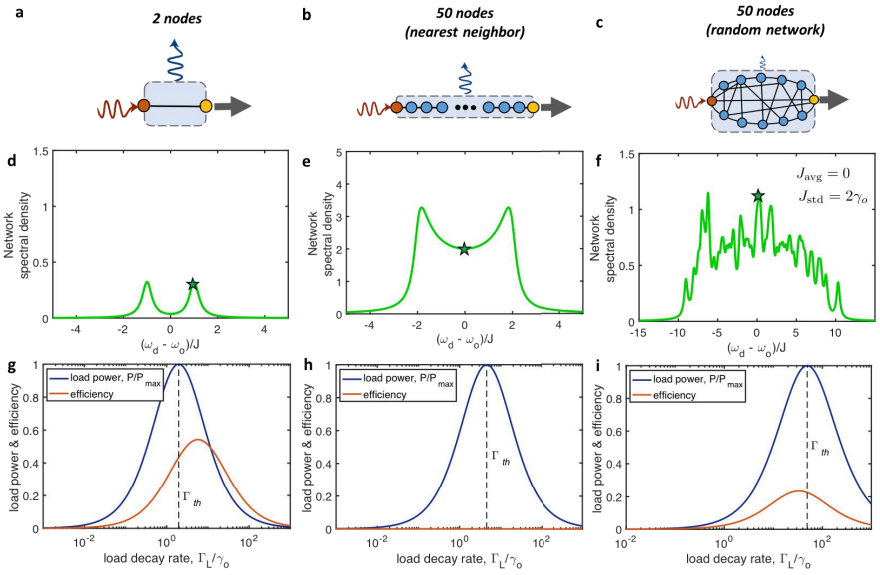

Fig. 2. Demonstration of quantum maximum power transfer theorem for three distinct networks: (a) 2-node network, (b) 50-node nearest neighbor network, (c) 50-node network with random all-to-all connectivity. (d)-(f) Network spectral density as a function of the input drive frequency ω. All nodes are assumed to have resonant frequency ω_o. The network spectral density shows the relative importance of different spectral modes within the network, and is closely related to the transmission amplitude used in input-output theory. (g)-(i) Numerical simulations of the load power and efficiency as a function of load decay rate. Each network is driven by a coherent field with driving frequency, $\omega_d = \{\omega_o + J, \omega_o, \omega_o\}$, denoted by the green stars in (d)-(f). Note the numerical simulations show excellent agreement with the quantum impedance matching condition Eq. (17).

The network spectral density in Figs. 2(e)-(f) show the relative magnitudes of the network's eigenmodes. For the two-node network shown in Fig. 2(a), there exists two dominant modes known as the symmetric and anti-symmetric modes with resonant frequencies $\omega_o + J$ and $\omega_o - J$ respectively (see Fig. 2(d). Furthermore, a driving field with frequency ω_d can be used to couple to a particular eigenstate of the network. In Figs. 2(g)-(i), we simulate driving the quantum network with different frequencies for each network, highlighted by the green stars in Fig. 2(d)-(f). By using the quantum impedance matching condition Eq. (17) as well as the Thevenin equivalent self-energy Eq. (13), we are able to calculate the optimal load decay rate where maximum power transfer occurs. The optimal load decay rates predicted by Eq. (13) and Eq. (17) are given by the

Optics EXPRESS

vertical dashed lines in Figs. 2(g)-(i). As expected, the exact analytical expressions match exactly with full numerical simulations.

8. Conclusion

In summary, we have presented the quantum analog of the maximum power transfer theorem for an N-node bosonic network. In recent years, research into energy transfer through complex networks, such as those arising in photosynthesis, have led to the development of reconfigurable and programmable energy transport simulators [15,16,22,30,31,40,41]. This work can therefore be tested immediately with reprogrammable photonic networks or other quantum simulators of bosonic systems. Finally, while this work provides a simple rule of thumb for linear networks, the role of nonlinearity as seen in Bose-Hubbard Hamiltonian models [42–45] requires additional considerations which should be studied carefully in the near future.

Appendix A: Power and efficiency

The power flow through the system is obtained from the Hamiltonian equation of motion Eq. (2):

$$\partial_t\langle H\rangle = \mathrm{tr}(\dot{H}\rho) + \mathrm{tr}(H\dot{\rho}) = P_{in} - P_{out}, \tag{20}$$

where ρ is the density matrix of the network and H is given by Eq. (1). The first term is the input power,

$$P_{in} = \mathrm{tr}(\dot{H}\rho) = i\omega_d \sum_n [\Omega_n\langle a_n\rangle e^{i\omega_d t} - \Omega_n^*\langle a_n^\dagger\rangle e^{-i\omega_d t}], \tag{21}$$

representing the work done by the driving field. The second term in Eq. (20) represents the output power,

$$P_{out} = -\mathrm{tr}(H\dot{\rho}) = -\mathrm{tr}(H\mathcal{D}_R[\rho]) - \mathrm{tr}(H\mathcal{D}_L[\rho]), \tag{22}$$

representing the total dissipated power of the network. It is possible to decompose the output power into two contributions. The first part is the power lost to some background reservoir,

$$P_R = -\mathrm{tr}(H\mathcal{D}_R[\rho]) \tag{23}$$

$$= \tfrac{1}{2}\sum_{n,m}\omega_{nm}(\gamma_n+\gamma_m)\langle a_n^\dagger a_m\rangle + \tfrac{1}{2}\sum_n \gamma_n(\Omega_n e^{i\omega_d t}\langle a_n\rangle + \Omega_n^* e^{-i\omega_d t}\langle a_n^\dagger\rangle). \tag{24}$$

For notational purposes, we have introduced $\omega_{nm} = \tilde{\omega}_n\delta_{nm} + J_{nm}(1-\delta_{nm})$. The second contribution corresponds to the power that is dissipated directly into the *load*,

$$P_L = -\mathrm{tr}(H\mathcal{D}_L[\rho]) \tag{25}$$

$$= \tfrac{1}{2}\sum_{n,m}\omega_{nm}(\Gamma_n+\Gamma_m)\langle a_n^\dagger a_m\rangle + \tfrac{1}{2}\sum_n \Gamma_n(\Omega_n e^{i\omega_d t}\langle a_n\rangle + \Omega_n^* e^{-i\omega_d t}\langle a_n^\dagger\rangle). \tag{26}$$

In matrix form, these equations may be written as:

$$P_R = \tfrac{1}{2}\tilde{\mathbf{a}}^\dagger\cdot(\boldsymbol{\mathcal{E}}\boldsymbol{\Gamma}_R + \boldsymbol{\Gamma}_R\boldsymbol{\mathcal{E}})\cdot\tilde{\mathbf{a}} + \tfrac{1}{2}(\boldsymbol{\Omega}^T\cdot\boldsymbol{\Gamma}_R\cdot\tilde{\mathbf{a}} + \tilde{\mathbf{a}}^\dagger\cdot\boldsymbol{\Gamma}_R\cdot\boldsymbol{\Omega}^*), \tag{27}$$

$$P_L = \tfrac{1}{2}\tilde{\mathbf{a}}^\dagger\cdot(\boldsymbol{\mathcal{E}}\boldsymbol{\Gamma}_L + \boldsymbol{\Gamma}_L\boldsymbol{\mathcal{E}})\cdot\tilde{\mathbf{a}} + \tfrac{1}{2}(\boldsymbol{\Omega}^T\cdot\boldsymbol{\Gamma}_L\cdot\tilde{\mathbf{a}} + \tilde{\mathbf{a}}^\dagger\cdot\boldsymbol{\Gamma}_L\cdot\boldsymbol{\Omega}^*). \tag{28}$$

For the rest of this document, we will only consider the steady-state limit, $\partial_t\langle H\rangle = 0$.

Optics EXPRESS

Appendix B: Quantum network equations of motion

To find the steady-state observables $\langle a_n^\dagger a_m\rangle_{ss}$ and $\langle a_n\rangle_{ss}$, we use Eq. (2) to derive the corresponding equations of motion,

$$\partial_t\langle a_n\rangle = i\sum_k(\mathcal{H}_{nk} + i\frac{\Gamma_n}{2}\delta_{nk})\langle a_k\rangle - i\Omega_n^* e^{-i\omega_d t}, \tag{29}$$

$$\begin{aligned}\partial_t\langle a_n^\dagger a_m\rangle = i\sum_k\Big[&(\mathcal{H}_{mk} + i\frac{\Gamma_m}{2}\delta_{mk})\langle a_n^\dagger a_k\rangle - (\mathcal{H}_{kn}^* - i\frac{\Gamma_k}{2}\delta_{kn})\langle a_k^\dagger a_m\rangle\Big]\\ &+ i[\Omega_n e^{+i\omega_d t}\langle a_m\rangle - \Omega_m^* e^{-i\omega_d t}\langle a_n^\dagger\rangle],\end{aligned} \tag{30}$$

where we have introduced the non-hermitian operator $\mathcal{H}_{nm} = -\omega_{nm} + i\frac{\gamma_n}{2}\delta_{nm}$. Note that this notation for the Hamiltonian is different by a factor i from those in the main text. To obtain the steady-state limit, we transform the equations of motion to the interaction picture using the substitution,

$$\langle a_m\rangle = \langle\tilde{a}_m\rangle e^{-i\omega_d t}, \tag{31}$$

giving

$$\partial_t\langle\tilde{a}_n\rangle = i\sum_k(\tilde{\mathcal{H}}_{nk} + i\frac{\Gamma_n}{2}\delta_{nk})\langle\tilde{a}_k\rangle - i\Omega_n^*, \tag{32}$$

$$\begin{aligned}\partial_t\langle\tilde{a}_n^\dagger\tilde{a}_m\rangle = i\sum_k\Big[&(\tilde{\mathcal{H}}_{mk} + i\frac{\Gamma_m}{2}\delta_{mk})\langle\tilde{a}_n^\dagger\tilde{a}_k\rangle - (\tilde{\mathcal{H}}_{kn}^* - i\frac{\Gamma_k}{2}\delta_{kn})\langle\tilde{a}_k^\dagger\tilde{a}_m\rangle\Big]\\ &+ i[\Omega_n\langle\tilde{a}_m\rangle - \Omega_m^*\langle\tilde{a}_n^\dagger\rangle],\end{aligned} \tag{33}$$

where $\tilde{\mathcal{H}}_{nm} = \mathcal{H}_{nm} + \delta_{nm}\omega_d$ with δ_{nm} as the kronecker delta function. In the large time limit, $t\to\infty$, the steady-state equations are given by,

$$0 = i\sum_k(\tilde{\mathcal{H}}_{nk} + i\frac{\Gamma_n}{2}\delta_{nk})\langle\tilde{a}_k\rangle - i\Omega_n^*, \tag{34}$$

$$\begin{aligned}0 = i\sum_k\Big[&(\tilde{\mathcal{H}}_{mk} + i\frac{\Gamma_m}{2}\delta_{mk})\langle\tilde{a}_n^\dagger\tilde{a}_k\rangle - (\tilde{\mathcal{H}}_{kn}^* - i\frac{\Gamma_k}{2}\delta_{kn})\langle\tilde{a}_k^\dagger\tilde{a}_m\rangle\Big]\\ &+ i[\Omega_n\langle\tilde{a}_m\rangle - \Omega_m^*\langle\tilde{a}_n^\dagger\rangle].\end{aligned} \tag{35}$$

These equations allow further simplification of the radiated and load power. After a bit of algebra, we obtain Eq. (6,7) in the main text,

$$P_L = \tfrac{1}{2}\sum_{n,m}(\Gamma_n + \Gamma_m)\left[\omega_{nm}\langle a_n^\dagger a_m\rangle + \Delta_{nm}\langle a_n^\dagger\rangle\langle a_m\rangle\right], \tag{36}$$

$$P_R = \tfrac{1}{2}\sum_{n,m}(\gamma_n + \gamma_m)\left[\omega_{nm}\langle a_n^\dagger a_m\rangle + \Delta_{nm}\langle a_n^\dagger\rangle\langle a_m\rangle\right]. \tag{37}$$

Coherent quantum network

In the absence of dephasing or coupling to a thermal bath, the coherent drive implies the factorization condition, $\langle a_n^\dagger a_m\rangle = \langle a_n^\dagger\rangle\langle a_m\rangle$, is exact. This is readily confirmed by comparing

Optics EXPRESS

Eqs. (29) and (30). In this limit, all relevant observables are obtained by solving Eq. (29) alone. Accordingly, it is straightforward to show that the radiated and load power simplify to:

$$P_L = \omega_d \sum_n \Gamma_n \langle a_n^\dagger \rangle \langle a_n \rangle, \tag{38}$$

$$P_R = \omega_d \sum_n \gamma_n \langle a_n^\dagger \rangle \langle a_n \rangle. \tag{39}$$

Note that both of these expressions are proportional to the driving frequency ω_d, which is an expected result in the classical description of driven harmonic oscillators. In the following sections, we will provide a proof of the maximum power transfer theorem for this purely coherent network.

Appendix C: Maximum power transfer

The maximum power transfer condition is derived by maximizing the load power. In matrix form, the load power is

$$P_L = \omega_d \left(\tilde{\mathbf{a}}^\dagger \mathbf{\Gamma}_L \tilde{\mathbf{a}} \right), \tag{40}$$

where $\tilde{\mathbf{a}} = (\langle \tilde{a}_1 \rangle, \ldots, \langle \tilde{a}_N \rangle)^T$ is an $N \times 1$ vector representing the node amplitudes in the rotating frame of the driving field. $\mathbf{\Gamma}_L$ is a diagonal matrix representing the dissipative coupling into the load. In matrix form, the amplitudes are constrained by Eq. (34),

$$i\mathbf{\Omega} = \boldsymbol{\mathcal{H}}\, \tilde{\mathbf{a}}, \tag{41}$$

as well as a positive semi-definite constraint on the load decay rate matrix. We have introduced the non-Hermitian matrix, $\boldsymbol{\mathcal{H}} = \tilde{\boldsymbol{\mathcal{H}}}_R + \boldsymbol{\mathcal{H}}_L$, composed of the bare non-Hermitian Hamiltonian defined in the absence of the load, $\tilde{\boldsymbol{\mathcal{H}}}_R$, with matrix elements, $[\tilde{\boldsymbol{\mathcal{H}}}_R]_{nm} = i\delta_{nm}(\omega_d - \omega_n + J_{nm}) - iJ_{nm} - \delta_{nm}\gamma_{nm}/2$. We have also defined the non-Hermitian matrix, $\boldsymbol{\mathcal{H}}_L = i\mathbf{\Lambda}_L - \mathbf{\Gamma}_L$, which is a diagonal matrix representing the non-Hermitian coupling to the load. Here, $\mathbf{\Lambda_L}$ is a diagonal matrix representing the Lamb shift $[\mathbf{\Lambda_L}]_{nm} = -\delta\omega_n\delta_{nm}$. The matrix form of these equations simplifies the analysis substantially. For example, the solution of Eq. (41) is given by, $\tilde{\mathbf{a}} = i\boldsymbol{\mathcal{H}}^{-1}\mathbf{\Omega}$, resulting in the following form for the load power,

$$P_L = \omega_d \left(\mathbf{\Omega}^\dagger \boldsymbol{\mathcal{H}}^{\dagger -1} \mathbf{\Gamma}_L \boldsymbol{\mathcal{H}}^{-1} \mathbf{\Omega} \right). \tag{42}$$

The conditions for maximum power are determined by the stationary points satisfying the system of equations,

$$\frac{\partial P_L}{\partial \omega_{L,i}} = 0 \quad \text{and} \quad \frac{\partial P_L}{\partial \Gamma_{L,i}} = 0, \tag{43}$$

where Lamb shift $\omega_{L,i} = [\mathbf{\Lambda_L}]_{ii}$ and dissipative coupling to the load $\Gamma_{L,i} = [\mathbf{\Gamma_L}]_{ii}/2$. Equation (43) may be written explicitly as,

$$\mathbf{\Omega}^\dagger \boldsymbol{\mathcal{H}}^{\dagger -1} \left(-\frac{\partial \boldsymbol{\mathcal{H}}_L^\dagger}{\partial \omega_{L,i}} \boldsymbol{\mathcal{H}}^{\dagger -1} \mathbf{\Gamma}_L - \mathbf{\Gamma}_L \boldsymbol{\mathcal{H}}^{-1} \frac{\partial \boldsymbol{\mathcal{H}}_L}{\partial \omega_{L,i}} \right) \boldsymbol{\mathcal{H}}^{-1} \mathbf{\Omega} = 0, \tag{44}$$

$$\mathbf{\Omega}^\dagger \boldsymbol{\mathcal{H}}^{\dagger -1} \left(-\frac{\partial \boldsymbol{\mathcal{H}}_L^\dagger}{\partial \Gamma_{L,i}} \boldsymbol{\mathcal{H}}^{\dagger -1} \mathbf{\Gamma}_L - \mathbf{\Gamma}_L \boldsymbol{\mathcal{H}}^{-1} \frac{\partial \boldsymbol{\mathcal{H}}_L}{\partial \Gamma_{L,i}} + \frac{\partial \mathbf{\Gamma}_L}{\partial \Gamma_{L,i}} \right) \boldsymbol{\mathcal{H}}^{-1} \mathbf{\Omega} = 0. \tag{45}$$

The matrix derivatives can be written as:

$$\frac{\partial \boldsymbol{\mathcal{H}}_L}{\partial \omega_{L,i}} = iP_i\,, \quad \frac{\partial \boldsymbol{\mathcal{H}}_L^\dagger}{\partial \omega_{L,i}} = -iP_i\,, \quad \frac{\partial \boldsymbol{\mathcal{H}}_L}{\partial \Gamma_{L,i}} = -P_i\,, \quad \frac{\partial \boldsymbol{\mathcal{H}}_L^\dagger}{\partial \Gamma_{L,i}} = -P_i\,, \quad \frac{\partial \mathbf{\Gamma}_L}{\partial \Gamma_{L,i}} = +P_i\,, \tag{46}$$

where P_i is a projection matrix with a single non-zero matrix element in the diagonal, δ_{ii}, corresponding the location of the ith node. This allows us to substitute Eq. (44) into Eq. (45),

Optics EXPRESS

resulting in following optimization condition for the ith node,

$$\boldsymbol{\Omega}^{\dagger}\boldsymbol{\mathcal{H}}^{\dagger-1}\left(2\boldsymbol{\Gamma}_L\boldsymbol{\mathcal{H}}^{-1}P_i + P_i\right)\boldsymbol{\mathcal{H}}^{-1}\boldsymbol{\Omega} = 0. \tag{47}$$

These are the defining set of equations for maximum power transfer. While these equations can be solved using numerical approaches, we are primarily interested in analytical solutions which can give rise to physical insights of the system. Generally, we were not able to find an analytical solution other than the defining case where a single node is coupled to the load.

Solvable conditions

In the single-node case, it is possible to show that a single unique and maximum solution exists. However, since the optimization problem is non-convex, we do not have any guarantees that there is a single maximum power transfer solution for the case of $k \geq 1$ nodes. This implies that conjugate impedance matching condition is generally not sufficient for solving this problem for the multiple node case ($k \geq 1$). Note that if the load represents a common reservoir, then it will induce off-diagonal coupling between the different nodes, implying that it may be possible to satisfy the maximum power condition. However, if the problem is given by k independent load reservoirs, then the solvable becomes non-linear and unsolvable using conjugate impedance matching alone.

Finally, we should point out that these results suggest that a more general load Hamiltonian, including off-diagonal components, may pave the way towards a solvable result. Physically, a load Hamiltonian with complex off-diagonal entries arises when multiple nodes are coupled to a common bath.

Thevenin equivalent network

The above result shows that optimal power transfer occurs when the load parameters are conjugately matched to the matrix, $\boldsymbol{\mathcal{H}}_{th}$, however, it remains unclear whether this matrix represents anything meaningful. In the following, we show that this matrix represents the effective non-Hermitian Hamiltonian of a k-node network coupled to the load. Starting from Eq. (41), the equation can be partitioned into the following set of coupled matrix equations:

$$i\boldsymbol{\Omega}_{k'} = \boldsymbol{\mathcal{H}}_{R,k'k'}\,\tilde{\mathbf{a}}_{k'} + \boldsymbol{\mathcal{H}}_{R,k'k}\,\tilde{\mathbf{a}}_{k}, \tag{48}$$

$$i\boldsymbol{\Omega}_{k} = \boldsymbol{\mathcal{H}}_{R,kk'}\,\tilde{\mathbf{a}}_{k'} + (\boldsymbol{\mathcal{H}}_{R,kk} + \boldsymbol{\mathcal{H}}_{k})\,\tilde{\mathbf{a}}_{k}. \tag{49}$$

Here, we have defined the set of indices k that represent the nodes coupled to the load, as well as indices k' that represent nodes uncoupled to the load. Here, $\boldsymbol{\Omega}_k$ and $\tilde{\mathbf{a}}_k$ are $k \times 1$ column vectors while $\boldsymbol{\Omega}_{k'}$ and $\tilde{\mathbf{a}}_{k'}$ are $(N-k) \times 1$ column vectors. Solving for $\tilde{\mathbf{a}}_{k'}$ in the first equation and substituting the result into the second equation,

$$i\boldsymbol{\Omega}_{th} = (\boldsymbol{\mathcal{H}}_{th} + \boldsymbol{\mathcal{H}}_{k})\,\tilde{\mathbf{a}}_{k}. \tag{50}$$

This equation is the defining equation for the Thevenin equivalent k-node network. The renormalized parameters of the Thevenin network are given by:

$$\boldsymbol{\Omega}_{th} = \boldsymbol{\Omega}_{k} - \boldsymbol{\mathcal{H}}_{R,kk'}\boldsymbol{\mathcal{H}}^{-1}_{R,k'k'}\boldsymbol{\Omega}_{k'}, \tag{51}$$

$$\boldsymbol{\mathcal{H}}_{th} = \boldsymbol{\mathcal{H}}_{R,kk} - \boldsymbol{\mathcal{H}}_{R,kk'}\boldsymbol{\mathcal{H}}^{-1}_{R,k'k'}\boldsymbol{\mathcal{H}}_{R,k'k}. \tag{52}$$

Using well-known results for the inverse of a 2×2 block matrix, it is possible to show that Eq. (49) and Eq. (50) are equivalent.

Optics EXPRESS

Appendix D: Hessian matrix

The maximum power transfer condition is derived by maximizing the load power. In matrix form, the load power is given by,

$$P_L = \omega_d \left(\tilde{\mathbf{a}}^\dagger \boldsymbol{\Gamma}_L \tilde{\mathbf{a}}\right) = \omega_d \left(\boldsymbol{\Omega}^\dagger \boldsymbol{\mathcal{H}}^{\dagger -1} \boldsymbol{\Gamma}_L \boldsymbol{\mathcal{H}}^{-1} \boldsymbol{\Omega}\right). \tag{53}$$

From before, recall that the first order derivatives may be written as,

$$\frac{\partial P_L}{\partial \omega_{L,i}} = \boldsymbol{\Omega}^\dagger \boldsymbol{\mathcal{H}}^{\dagger -1} \left(-\frac{\partial \boldsymbol{\mathcal{H}}_L^\dagger}{\partial \omega_{L,i}} \boldsymbol{\mathcal{H}}^{\dagger -1} \boldsymbol{\Gamma}_L - \boldsymbol{\Gamma}_L \boldsymbol{\mathcal{H}}^{-1} \frac{\partial \boldsymbol{\mathcal{H}}_L}{\partial \omega_{L,i}} \right) \boldsymbol{\mathcal{H}}^{-1} \boldsymbol{\Omega}, \tag{54}$$

$$\frac{\partial P_L}{\partial \Gamma_{L,i}} = \boldsymbol{\Omega}^\dagger \boldsymbol{\mathcal{H}}^{\dagger -1} \left(-\frac{\partial \boldsymbol{\mathcal{H}}_L^\dagger}{\partial \Gamma_{L,i}} \boldsymbol{\mathcal{H}}^{\dagger -1} \boldsymbol{\Gamma}_L - \boldsymbol{\Gamma}_L \boldsymbol{\mathcal{H}}^{-1} \frac{\partial \boldsymbol{\mathcal{H}}_L}{\partial \Gamma_{L,i}} + \frac{\partial \boldsymbol{\Gamma}_L}{\partial \Gamma_{L,i}} \right) \boldsymbol{\mathcal{H}}^{-1} \boldsymbol{\Omega}, \tag{55}$$

where we again use:

$$\frac{\partial \boldsymbol{\mathcal{H}}_L}{\partial \omega_{L,i}} = iP_i \,, \quad \frac{\partial \boldsymbol{\mathcal{H}}_L^\dagger}{\partial \omega_{L,i}} = -iP_i \,, \quad \frac{\partial \boldsymbol{\mathcal{H}}_L}{\partial \Gamma_{L,i}} = -P_i \,, \quad \frac{\partial \boldsymbol{\mathcal{H}}_L^\dagger}{\partial \Gamma_{L,i}} = -P_i \,, \quad \frac{\partial \boldsymbol{\Gamma}_L}{\partial \Gamma_{L,i}} = +P_i \,, \tag{56}$$

where P_i is a projection matrix with a single non-zero matrix element in the diagonal, δ_{ii}, corresponding the location of the ith node. This allows us to write the first order derivative with respect to the decay rate as:

$$\frac{\partial P_L}{\partial \Gamma_{L,i}} = \boldsymbol{\Omega}^\dagger \boldsymbol{\mathcal{H}}^{\dagger -1} \left(P_i \boldsymbol{\mathcal{H}}^{\dagger -1} \boldsymbol{\Gamma}_L + \boldsymbol{\Gamma}_L \boldsymbol{\mathcal{H}}^{-1} P_i + P_i \right) \boldsymbol{\mathcal{H}}^{-1} \boldsymbol{\Omega}. \tag{57}$$

The second order derivative with respect to the decay rate is then given by:

$$\begin{aligned}
\frac{\partial^2 P_L}{\partial \Gamma_{L,j} \partial \Gamma_{L,i}} &= \frac{\partial}{\partial \Gamma_{L,j}} (\boldsymbol{\Omega}^\dagger \boldsymbol{\mathcal{H}}^{\dagger -1} P_i \boldsymbol{\mathcal{H}}^{\dagger -1} \boldsymbol{\Gamma}_L \boldsymbol{\mathcal{H}}^{-1} \boldsymbol{\Omega} \\
&\quad + \boldsymbol{\Omega}^\dagger \boldsymbol{\mathcal{H}}^{\dagger -1} \boldsymbol{\Gamma}_L \boldsymbol{\mathcal{H}}^{-1} P_i \boldsymbol{\mathcal{H}}^{-1} \boldsymbol{\Omega} + \boldsymbol{\Omega}^\dagger \boldsymbol{\mathcal{H}}^{\dagger -1} P_i \boldsymbol{\mathcal{H}}^{-1} \boldsymbol{\Omega}) \\
&= \boldsymbol{\Omega}^\dagger \boldsymbol{\mathcal{H}}^{\dagger -1} P_j \boldsymbol{\mathcal{H}}^{\dagger -1} P_i \boldsymbol{\mathcal{H}}^{\dagger -1} \boldsymbol{\Gamma}_L \boldsymbol{\mathcal{H}}^{-1} \boldsymbol{\Omega} + \boldsymbol{\Omega}^\dagger \boldsymbol{\mathcal{H}}^{\dagger -1} P_i \boldsymbol{\mathcal{H}}^{\dagger -1} P_j \boldsymbol{\mathcal{H}}^{\dagger -1} \boldsymbol{\Gamma}_L \boldsymbol{\mathcal{H}}^{-1} \boldsymbol{\Omega} \\
&\quad + \boldsymbol{\Omega}^\dagger \boldsymbol{\mathcal{H}}^{\dagger -1} P_i \boldsymbol{\mathcal{H}}^{\dagger -1} P_j \boldsymbol{\mathcal{H}}^{-1} \boldsymbol{\Omega} + \boldsymbol{\Omega}^\dagger \boldsymbol{\mathcal{H}}^{\dagger -1} P_i \boldsymbol{\mathcal{H}}^{\dagger -1} \boldsymbol{\Gamma}_L \boldsymbol{\mathcal{H}}^{-1} P_j \boldsymbol{\mathcal{H}}^{-1} \boldsymbol{\Omega} \\
&\quad + \boldsymbol{\Omega}^\dagger \boldsymbol{\mathcal{H}}^{\dagger -1} P_j \boldsymbol{\mathcal{H}}^{\dagger -1} \boldsymbol{\Gamma}_L \boldsymbol{\mathcal{H}}^{-1} P_i \boldsymbol{\mathcal{H}}^{-1} \boldsymbol{\Omega} + \boldsymbol{\Omega}^\dagger \boldsymbol{\mathcal{H}}^{\dagger -1} P_j \boldsymbol{\mathcal{H}}^{-1} P_i \boldsymbol{\mathcal{H}}^{-1} \boldsymbol{\Omega} \\
&\quad + \boldsymbol{\Omega}^\dagger \boldsymbol{\mathcal{H}}^{\dagger -1} \boldsymbol{\Gamma}_L \boldsymbol{\mathcal{H}}^{-1} P_j \boldsymbol{\mathcal{H}}^{-1} P_i \boldsymbol{\mathcal{H}}^{-1} \boldsymbol{\Omega} + \boldsymbol{\Omega}^\dagger \boldsymbol{\mathcal{H}}^{\dagger -1} \boldsymbol{\Gamma}_L \boldsymbol{\mathcal{H}}^{-1} P_i \boldsymbol{\mathcal{H}}^{-1} P_j \boldsymbol{\mathcal{H}}^{-1} \boldsymbol{\Omega} \\
&\quad + \boldsymbol{\Omega}^\dagger \boldsymbol{\mathcal{H}}^{\dagger -1} P_j \boldsymbol{\mathcal{H}}^{\dagger -1} P_i \boldsymbol{\mathcal{H}}^{-1} \boldsymbol{\Omega} + \boldsymbol{\Omega}^\dagger \boldsymbol{\mathcal{H}}^{\dagger -1} P_i \boldsymbol{\mathcal{H}}^{-1} P_j \boldsymbol{\mathcal{H}}^{-1} \boldsymbol{\Omega}.
\end{aligned} \tag{58}$$

Grouping the outer terms, we can write:

$$\begin{aligned}
\frac{\partial^2 P_L}{\partial \Gamma_{L,j} \partial \Gamma_{L,i}} &= \boldsymbol{\Omega}^\dagger \boldsymbol{\mathcal{H}}^{\dagger -1} \Big(P_j \boldsymbol{\mathcal{H}}^{\dagger -1} P_i \boldsymbol{\mathcal{H}}^{\dagger -1} \boldsymbol{\Gamma}_L + P_i \boldsymbol{\mathcal{H}}^{\dagger -1} P_j \boldsymbol{\mathcal{H}}^{\dagger -1} \boldsymbol{\Gamma}_L + P_i \boldsymbol{\mathcal{H}}^{\dagger -1} P_j \\
&\quad + P_i \boldsymbol{\mathcal{H}}^{\dagger -1} \boldsymbol{\Gamma}_L \boldsymbol{\mathcal{H}}^{-1} P_j + P_j \boldsymbol{\mathcal{H}}^{\dagger -1} \boldsymbol{\Gamma}_L \boldsymbol{\mathcal{H}}^{-1} P_i + P_j \boldsymbol{\mathcal{H}}^{-1} P_i + \boldsymbol{\Gamma}_L \boldsymbol{\mathcal{H}}^{-1} P_j \boldsymbol{\mathcal{H}}^{-1} P_i \\
&\quad + \boldsymbol{\Gamma}_L \boldsymbol{\mathcal{H}}^{-1} P_i \boldsymbol{\mathcal{H}}^{-1} P_j + P_j \boldsymbol{\mathcal{H}}^{\dagger -1} P_i + P_i \boldsymbol{\mathcal{H}}^{-1} P_j \Big) \boldsymbol{\mathcal{H}}^{-1} \boldsymbol{\Omega}.
\end{aligned} \tag{59}$$

The first order derivative with respect to the Lamb shift is given by:

$$\frac{\partial P_L}{\partial \omega_{L,i}} = i\boldsymbol{\Omega}^\dagger \boldsymbol{\mathcal{H}}^{\dagger -1} \left(P_i \boldsymbol{\mathcal{H}}^{\dagger -1} \boldsymbol{\Gamma}_L - \boldsymbol{\Gamma}_L \boldsymbol{\mathcal{H}}^{-1} P_i \right) \boldsymbol{\mathcal{H}}^{-1} \boldsymbol{\Omega}. \tag{60}$$

Optics EXPRESS

Likewise, the second order derivative with respect to the Lamb shift is given by:

$$\begin{aligned}\frac{\partial^2 P_L}{\partial\omega_{L,j}\partial\omega_{L,i}} &= \frac{\partial}{\partial\omega_{L,j}} i\boldsymbol{\Omega}^\dagger\boldsymbol{\mathcal{H}}^{\dagger-1}\left(P_i\boldsymbol{\mathcal{H}}^{\dagger-1}\boldsymbol{\Gamma}_L - \boldsymbol{\Gamma}_L\boldsymbol{\mathcal{H}}^{-1}P_i\right)\boldsymbol{\mathcal{H}}^{-1}\boldsymbol{\Omega}\\ &= \boldsymbol{\Omega}^\dagger\boldsymbol{\mathcal{H}}^{\dagger-1}P_j\boldsymbol{\mathcal{H}}^{\dagger-1}\left(P_i\boldsymbol{\mathcal{H}}^{\dagger-1}\boldsymbol{\Gamma}_L - \boldsymbol{\Gamma}_L\boldsymbol{\mathcal{H}}^{-1}P_i\right)\boldsymbol{\mathcal{H}}^{-1}\boldsymbol{\Omega}\\ &+ \boldsymbol{\Omega}^\dagger\boldsymbol{\mathcal{H}}^{\dagger-1}\left(P_i\boldsymbol{\mathcal{H}}^{\dagger-1}P_j\boldsymbol{\mathcal{H}}^{\dagger-1}\boldsymbol{\Gamma}_L + \boldsymbol{\Gamma}_L\boldsymbol{\mathcal{H}}^{-1}P_j\boldsymbol{\mathcal{H}}^{-1}P_i\right)\boldsymbol{\mathcal{H}}^{-1}\boldsymbol{\Omega}\\ &- \boldsymbol{\Omega}^\dagger\boldsymbol{\mathcal{H}}^{\dagger-1}\left(P_i\boldsymbol{\mathcal{H}}^{\dagger-1}\boldsymbol{\Gamma}_L - \boldsymbol{\Gamma}_L\boldsymbol{\mathcal{H}}^{-1}P_i\right)\boldsymbol{\mathcal{H}}^{-1}P_j\boldsymbol{\mathcal{H}}^{-1}\boldsymbol{\Omega}.\end{aligned} \tag{61}$$

Grouping the outer terms, we can write:

$$\begin{aligned}\frac{\partial^2 P_L}{\partial\omega_{L,j}\partial\omega_{L,i}} &= \boldsymbol{\Omega}^\dagger\boldsymbol{\mathcal{H}}^{\dagger-1}\Big(P_j\boldsymbol{\mathcal{H}}^{\dagger-1}P_i\boldsymbol{\mathcal{H}}^{\dagger-1}\boldsymbol{\Gamma}_L - P_j\boldsymbol{\mathcal{H}}^{\dagger-1}\boldsymbol{\Gamma}_L\boldsymbol{\mathcal{H}}^{-1}P_i\\ &+ P_i\boldsymbol{\mathcal{H}}^{\dagger-1}P_j\boldsymbol{\mathcal{H}}^{\dagger-1}\boldsymbol{\Gamma}_L + \boldsymbol{\Gamma}_L\boldsymbol{\mathcal{H}}^{-1}P_j\boldsymbol{\mathcal{H}}^{-1}P_i\\ &- P_i\boldsymbol{\mathcal{H}}^{\dagger-1}\boldsymbol{\Gamma}_L\boldsymbol{\mathcal{H}}^{-1}P_j + \boldsymbol{\Gamma}_L\boldsymbol{\mathcal{H}}^{-1}P_i\boldsymbol{\mathcal{H}}^{-1}P_j\Big)\boldsymbol{\mathcal{H}}^{-1}\boldsymbol{\Omega}.\end{aligned} \tag{62}$$

We now calculate the cross-terms. The first cross-term is given by:

$$\begin{aligned}\frac{\partial^2 P_L}{\partial\omega_{L,j}\partial\Gamma_{L,i}} &= \frac{\partial}{\partial\omega_{L,j}}\boldsymbol{\Omega}^\dagger\boldsymbol{\mathcal{H}}^{\dagger-1}\left(P_i\boldsymbol{\mathcal{H}}^{\dagger-1}\boldsymbol{\Gamma}_L + \boldsymbol{\Gamma}_L\boldsymbol{\mathcal{H}}^{-1}P_i + P_i\right)\boldsymbol{\mathcal{H}}^{-1}\boldsymbol{\Omega}\\ &= i\boldsymbol{\Omega}^\dagger\boldsymbol{\mathcal{H}}^{\dagger-1}P_j\boldsymbol{\mathcal{H}}^{\dagger-1}\left(P_i\boldsymbol{\mathcal{H}}^{\dagger-1}\boldsymbol{\Gamma}_L + \boldsymbol{\Gamma}_L\boldsymbol{\mathcal{H}}^{-1}P_i + P_i\right)\boldsymbol{\mathcal{H}}^{-1}\boldsymbol{\Omega}\\ &+ \boldsymbol{\Omega}^\dagger\boldsymbol{\mathcal{H}}^{\dagger-1}\left(iP_i\boldsymbol{\mathcal{H}}^{\dagger-1}P_j\boldsymbol{\mathcal{H}}^{\dagger-1}\boldsymbol{\Gamma}_L - i\boldsymbol{\Gamma}_L\boldsymbol{\mathcal{H}}^{-1}P_j\boldsymbol{\mathcal{H}}^{-1}P_i\right)\boldsymbol{\mathcal{H}}^{-1}\boldsymbol{\Omega}\\ &- i\boldsymbol{\Omega}^\dagger\boldsymbol{\mathcal{H}}^{\dagger-1}\left(P_i\boldsymbol{\mathcal{H}}^{\dagger-1}\boldsymbol{\Gamma}_L + \boldsymbol{\Gamma}_L\boldsymbol{\mathcal{H}}^{-1}P_i + P_i\right)\boldsymbol{\mathcal{H}}^{-1}P_j\boldsymbol{\mathcal{H}}^{-1}\boldsymbol{\Omega},\end{aligned} \tag{63}$$

where we factorize some terms to obtain:

$$\begin{aligned}\frac{\partial^2 P_L}{\partial\omega_{L,j}\partial\Gamma_{L,i}} &= i\boldsymbol{\Omega}^\dagger\boldsymbol{\mathcal{H}}^{\dagger-1}\Big(P_j\boldsymbol{\mathcal{H}}^{\dagger-1}P_i\boldsymbol{\mathcal{H}}^{\dagger-1}\boldsymbol{\Gamma}_L + P_j\boldsymbol{\mathcal{H}}^{\dagger-1}\boldsymbol{\Gamma}_L\boldsymbol{\mathcal{H}}^{-1}P_i + P_j\boldsymbol{\mathcal{H}}^{\dagger-1}P_i\\ &+ P_i\boldsymbol{\mathcal{H}}^{\dagger-1}P_j\boldsymbol{\mathcal{H}}^{\dagger-1}\boldsymbol{\Gamma}_L - \boldsymbol{\Gamma}_L\boldsymbol{\mathcal{H}}^{-1}P_j\boldsymbol{\mathcal{H}}^{-1}P_i\\ &- P_i\boldsymbol{\mathcal{H}}^{\dagger-1}\boldsymbol{\Gamma}_L\boldsymbol{\mathcal{H}}^{-1}P_j - \boldsymbol{\Gamma}_L\boldsymbol{\mathcal{H}}^{-1}P_i\boldsymbol{\mathcal{H}}^{-1}P_j - P_i\boldsymbol{\mathcal{H}}^{-1}P_j\Big)\boldsymbol{\mathcal{H}}^{-1}\boldsymbol{\Omega},\end{aligned} \tag{64}$$

as well as the other cross-term:

$$\begin{aligned}&\frac{\partial^2 P_L}{\partial\Gamma_{L,j}\partial\omega_{L,i}} = \frac{\partial}{\partial\Gamma_{L,j}} i\boldsymbol{\Omega}^\dagger\boldsymbol{\mathcal{H}}^{\dagger-1}\left(P_i\boldsymbol{\mathcal{H}}^{\dagger-1}\boldsymbol{\Gamma}_L - \boldsymbol{\Gamma}_L\boldsymbol{\mathcal{H}}^{-1}P_i\right)\boldsymbol{\mathcal{H}}^{-1}\boldsymbol{\Omega}\\ &= -i\boldsymbol{\Omega}^\dagger\boldsymbol{\mathcal{H}}^{\dagger-1}P_j\boldsymbol{\mathcal{H}}^{\dagger-1}\left(P_i\boldsymbol{\mathcal{H}}^{\dagger-1}\boldsymbol{\Gamma}_L - \boldsymbol{\Gamma}_L\boldsymbol{\mathcal{H}}^{-1}P_i\right)\boldsymbol{\mathcal{H}}^{-1}\boldsymbol{\Omega}\\ &+ i\boldsymbol{\Omega}^\dagger\boldsymbol{\mathcal{H}}^{\dagger-1}(-P_i\boldsymbol{\mathcal{H}}^{\dagger-1}P_j\boldsymbol{\mathcal{H}}^{\dagger-1}\boldsymbol{\Gamma}_L + P_i\boldsymbol{\mathcal{H}}^{\dagger-1}P_j - P_j\boldsymbol{\mathcal{H}}^{-1}P_i\\ &+ \boldsymbol{\Gamma}_L\boldsymbol{\mathcal{H}}^{-1}P_j\boldsymbol{\mathcal{H}}^{-1}P_i)\boldsymbol{\mathcal{H}}^{-1}\boldsymbol{\Omega} - i\boldsymbol{\Omega}^\dagger\boldsymbol{\mathcal{H}}^{\dagger-1}(P_i\boldsymbol{\mathcal{H}}^{\dagger-1}\boldsymbol{\Gamma}_L - \boldsymbol{\Gamma}_L\boldsymbol{\mathcal{H}}^{-1}P_i)\boldsymbol{\mathcal{H}}^{-1}P_j\boldsymbol{\mathcal{H}}^{-1}\boldsymbol{\Omega}.\end{aligned} \tag{65}$$

After factorization, we obtain:

$$\begin{aligned}\frac{\partial^2 P_L}{\partial\Gamma_{L,j}\partial\omega_{L,i}} &= i\boldsymbol{\Omega}^\dagger\boldsymbol{\mathcal{H}}^{\dagger-1}\Big(-P_j\boldsymbol{\mathcal{H}}^{\dagger-1}P_i\boldsymbol{\mathcal{H}}^{\dagger-1}\boldsymbol{\Gamma}_L + P_j\boldsymbol{\mathcal{H}}^{\dagger-1}\boldsymbol{\Gamma}_L\boldsymbol{\mathcal{H}}^{-1}P_i\\ &- P_i\boldsymbol{\mathcal{H}}^{\dagger-1}P_j\boldsymbol{\mathcal{H}}^{\dagger-1}\boldsymbol{\Gamma}_L + P_i\boldsymbol{\mathcal{H}}^{\dagger-1}P_j - P_j\boldsymbol{\mathcal{H}}^{-1}P_i + \boldsymbol{\Gamma}_L\boldsymbol{\mathcal{H}}^{-1}P_j\boldsymbol{\mathcal{H}}^{-1}P_i\\ &- P_i\boldsymbol{\mathcal{H}}^{\dagger-1}\boldsymbol{\Gamma}_L\boldsymbol{\mathcal{H}}^{-1}P_j + \boldsymbol{\Gamma}_L\boldsymbol{\mathcal{H}}^{-1}P_i\boldsymbol{\mathcal{H}}^{-1}P_j\Big)\boldsymbol{\mathcal{H}}^{-1}\boldsymbol{\Omega}.\end{aligned} \tag{66}$$

The only thing remaining here is to group the first and last terms in the last two expressions for simplification. The big results have been derived.

Optics EXPRESS

Appendix E: Network spectral density

To characterize different quantum networks, we use the network spectral density

$$S(\omega_d) = \mathrm{Im}[\mathrm{tr}(\omega_d - H_{eff})^{-1}]. \tag{67}$$

Note that this quantity may be related to the transmission,

$$t = \kappa\langle a\rangle/\Omega_1 = \frac{\kappa}{i\Delta + \kappa + g^2/(i\Delta + \gamma)}, \tag{68}$$

typically used in input-output theory [37].

Funding. Defense Advanced Research Projects Agency Nascent Light-Matter Interactions (NLM) Program.

Disclosures. The authors declare no conflicts of interest.

Data availability. Data underlying the results presented in this paper are not publicly available at this time but may be obtained from the authors upon reasonable request.

References

1. D. W. K. Ng, E. S. Lo, and R. Schober, "Wireless information and power transfer: Energy efficiency optimization in OFDMA systems," IEEE Trans. Wireless Commun. **12**(12), 6352–6370 (2013).
2. L. R. Varshney, "Transporting information and energy simultaneously," in *International Symposium on Information Theory* (IEEE, 2008), pp. 1612–1616.
3. P. Grover and A. Sahai, "Shannon meets Tesla: Wireless information and power transfer," in *International Symposium on Information Theory* (IEEE, 2010), pp. 2363–2367.
4. S. Rafiq and G. D. Scholes, "From fundamental theories to quantum coherences in electron transfer," J. Am. Chem. Soc. **141**(2), 708–722 (2019).
5. F. Caruso, A. W. Chin, A. Datta, S. F. Huelga, and M. B. Plenio, "Highly efficient energy excitation transfer in light-harvesting complexes: The fundamental role of noise-assisted transport," J. Chem. Phys. **131**(10), 105106 (2009).
6. A. W. Chin, A. Datta, F. Caruso, S. F. Huelga, and M. B. Plenio, "Noise-assisted energy transfer in quantum networks and light-harvesting complexes," New J. Phys. **12**(6), 065002 (2010).
7. A. Olaya-Castro, C. F. Lee, F. F. Olsen, and N. F. Johnson, "Efficiency of energy transfer in a light-harvesting system under quantum coherence," Phys. Rev. B **78**(8), 085115 (2008).
8. C. Blum, N. Zijlstra, A. Lagendijk, M. Wubs, A. P. Mosk, V. Subramaniam, and W. L. Vos, "Nanophotonic control of the förster resonance energy transfer efficiency," Phys. Rev. Lett. **109**(20), 203601 (2012).
9. W. D. Newman, C. L. Cortes, A. Afshar, K. Cadien, A. Meldrum, R. Fedosejevs, and Z. Jacob, "Observation of long-range dipole-dipole interactions in hyperbolic metamaterials," Sci. Adv. **4**(10), eaar5278 (2018).
10. R. Deshmukh, S.-A. Biehs, E. Khwaja, T. Galfsky, G. S. Agarwal, and V. M. Menon, "Long-range resonant energy transfer using optical topological transitions in metamaterials," ACS Photonics **5**(7), 2737–2741 (2018).
11. C. L. Cortes and Z. Jacob, "Fundamental figures of merit for engineering Förster resonance energy transfer," Opt. Express **26**(15), 19371–19387 (2018).
12. A. Kurs, A. Karalis, R. Moffatt, J. D. Joannopoulos, P. Fisher, and M. Soljacic, "Wireless power transfer via strongly coupled magnetic resonances," Science **317**(5834), 83–86 (2007).
13. X. Yu, T. Skauli, B. Skauli, S. Sandhu, P. B. Catrysse, and S. Fan, "Wireless power transfer in the presence of metallic plates: Experimental results," AIP Adv. **3**(6), 062102 (2013).
14. A. Krasnok, D. G. Baranov, A. Generalov, S. Li, and A. Alù, "Coherently enhanced wireless power transfer," Phys. Rev. Lett. **120**(14), 143901 (2018).
15. S. Viciani, M. Lima, M. Bellini, and F. Caruso, "Observation of noise-assisted transport in an all-optical cavity-based network," Phys. Rev. Lett. **115**(8), 083601 (2015).
16. S. Viciani, S. Gherardini, M. Lima, M. Bellini, and F. Caruso, "Disorder and dephasing as control knobs for light transport in optical fiber cavity networks," Sci. Rep. **6**(1), 37791 (2016).
17. M. Kim, Y. Choi, C. Yoon, W. Choi, J. Kim, Q.-H. Park, and W. Choi, "Maximal energy transport through disordered media with the implementation of transmission eigenchannels," Nat. Photonics **6**(9), 581–585 (2012).
18. S. Popoff, A. Goetschy, S. Liew, A. D. Stone, and H. Cao, "Coherent control of total transmission of light through disordered media," Phys. Rev. Lett. **112**(13), 133903 (2014).
19. Z. Shi and A. Z. Genack, "Transmission eigenvalues and the bare conductance in the crossover to Anderson localization," Phys. Rev. Lett. **108**(4), 043901 (2012).
20. P. Rebentrost, M. Mohseni, I. Kassal, S. Lloyd, and A. Aspuru-Guzik, "Environment-assisted quantum transport," New J. Phys. **11**(3), 033003 (2009).
21. G. S. Engel, T. R. Calhoun, E. L. Read, T.-K. Ahn, T. Mančal, Y.-C. Cheng, R. E. Blankenship, and G. R. Fleming, "Evidence for wavelike energy transfer through quantum coherence in photosynthetic systems," Nature **446**(7137), 782–786 (2007).

Optics EXPRESS

22. N. Trautmann and P. Hauke, "Trapped-ion quantum simulation of excitation transport: Disordered, noisy, and long-range connected quantum networks," Phys. Rev. A **97**(2), 023606 (2018).
23. W. W. Ho, S. Choi, M. D. Lukin, and D. A. Abanin, "Critical time crystals in dipolar systems," Phys. Rev. Lett. **119**(1), 010602 (2017).
24. G. Panitchayangkoon, D. V. Voronine, D. Abramavicius, J. R. Caram, N. H. Lewis, S. Mukamel, and G. S. Engel, "Direct evidence of quantum transport in photosynthetic light-harvesting complexes," Proc. Natl. Acad. Sci. **108**(52), 20908–20912 (2011).
25. J. Huber and P. Rabl, "Active energy transport and the role of symmetry breaking in microscopic power grids," Phys. Rev. A **100**(1), 012129 (2019).
26. I. Krikidis, S. Timotheou, S. Nikolaou, G. Zheng, D. W. K. Ng, and R. Schober, "Simultaneous wireless information and power transfer in modern communication systems," IEEE Commun. Mag. **52**(11), 104–110 (2014).
27. R. Zhang and C. K. Ho, "Mimo broadcasting for simultaneous wireless information and power transfer," IEEE Trans. Wireless Commun. **12**(5), 1989–2001 (2013).
28. C. Desoer, "The maximum power transfer theorem for n-ports," IEEE Trans. Circuit Theory **20**(3), 328–330 (1973).
29. R. Jozsa, "Fidelity for mixed quantum states," J. Mod. Opt. **41**(12), 2315–2323 (1994).
30. B.-X. Wang, M.-J. Tao, Q. Ai, T. Xin, N. Lambert, D. Ruan, Y.-C. Cheng, F. Nori, F.-G. Deng, and G.-L. Long, "Efficient quantum simulation of photosynthetic light harvesting," npj Quantum Inf. **4**(1), 52 (2018).
31. A. Chin, E. Mangaud, O. Atabek, and M. Desouter-Lecomte, "Coherent quantum dynamics launched by incoherent relaxation in a quantum circuit simulator of a light-harvesting complex," Phys. Rev. A **97**(6), 063823 (2018).
32. H.-P. Breuer and F. Petruccione, *The Theory of Open Quantum Systems* (Oxford University Press, 2007).
33. R. Kosloff, "Quantum thermodynamics: A dynamical viewpoint," Entropy **15**(12), 2100–2128 (2013).
34. R. Kosloff and A. Levy, "Quantum heat engines and refrigerators: Continuous devices," Annu. Rev. Phys. Chem. **65**(1), 365–393 (2014).
35. M. Simoncelli, N. Marzari, and F. Mauri, "Unified theory of thermal transport in crystals and glasses," Nat. Phys. **15**(8), 809–813 (2019).
36. J. Sherman and W. J. Morrison, "Adjustment of an inverse matrix corresponding to a change in one element of a given matrix," Ann. Math. Stat. **21**(1), 124–127 (1950).
37. D. Plankensteiner, C. Sommer, H. Ritsch, and C. Genes, "Cavity antiresonance spectroscopy of dipole coupled subradiant arrays," Phys. Rev. Lett. **119**(9), 093601 (2017).
38. R. Prabhu, S. Pradhan, A. Sen(De), and U. Sen, "Disorder overtakes order in information concentration over quantum networks," Phys. Rev. A **84**(4), 042334 (2011).
39. S. Perseguers, G. J. Lapeyre, D. Cavalcanti, M. Lewenstein, and A. Acín, "Distribution of entanglement in large-scale quantum networks," Rep. Prog. Phys. **76**(9), 096001 (2013).
40. A. Potočnik, A. Bargerbos, F. A. Schröder, S. A. Khan, M. C. Collodo, S. Gasparinetti, Y. Salathé, C. Creatore, C. Eichler, H. E. Türeci, A. W. Chin, and A. Wallraff, "Studying light-harvesting models with superconducting circuits," Nat. Commun. **9**(1), 904 (2018).
41. D. J. Gorman, B. Hemmerling, E. Megidish, S. A. Moeller, P. Schindler, M. Sarovar, and H. Haeffner, "Engineering vibrationally assisted energy transfer in a trapped-ion quantum simulator," Phys. Rev. X **8**(1), 011038 (2018).
42. T. D. Kühner and H. Monien, "Phases of the one-dimensional Bose-Hubbard model," Phys. Rev. B **58**(22), R14741(R) (1998).
43. K. Góral, L. Santos, and M. Lewenstein, "Quantum phases of dipolar bosons in optical lattices," Phys. Rev. Lett. **88**(17), 170406 (2002).
44. C. Kollath, A. M. Läuchli, and E. Altman, "Quench dynamics and nonequilibrium phase diagram of the Bose-Hubbard model," Phys. Rev. Lett. **98**(18), 180601 (2007).
45. P. Buonsante and A. Vezzani, "Ground-state fidelity and bipartite entanglement in the Bose-Hubbard model," Phys. Rev. Lett. **98**(11), 110601 (2007).

31.205.88.229 {ts '2022-09-21 14:54:27'}